10.1002/anie.202009719

WILEY-VCH

COMMUNICATION

Enantiospecific solid solution formation triggers the propagation of homochirality

Iaroslav Baglai,[a] Michel Leeman,[b] Klaus Wurst,[c] Richard M. Kellogg,[b] and Willem L. Noorduin*[a]

[a] Dr. I. Baglai, Dr. W. L. Noorduin
AMOLF, Science Park 104, 1098 XG Amsterdam, The Netherlands
E-mail: noorduin@amolf.nl
[b] Dr. M. Leeman, Prof. Dr. R. M. Kellogg
Syncom BV, Kadijk 3, 9747 AT Groningen, The Netherlands
[c] Dr. K. Wurst
University of Innsbruck, Innrain 80-82, A-6020 Innsbruck, Austria

Supporting information for this article is given via a link at the end of the document.

Abstract: *Propagation of homochirality plays a crucial role in the discussion on the origin of life. We here investigate the role of structurally related enantiopure additives in chiral symmetry breaking during reactive crystallizations. We demonstrate that a symmetry breaking process can be driven towards the same absolute configuration as the additive if this additive forms an enantiospecific solid solution with the racemate. We observe two antagonistic processes: enantiospecific growth inhibition directs symmetry breaking to the opposite enantiomer following "the rule of reversal" and enantiospecific solid solution formation that favors homochiral outcomes. During continuous grinding, contributions of solid solution formation override contributions of enantiospecific growth inhibition, directing the process towards the absolute configuration of the additive. Collectively, our findings offer a potential mechanism for propagation of homochirality.*

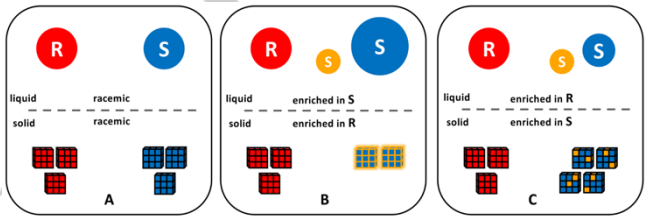

Figure 1. Multiple ways of an additive-driven chiral symmetry breaking. (A) Racemic conglomerate. (B) Additive (orange) showing enantiospecific growth inhibition with the enantiomer of the same absolute configuration, thus favoring the crystallization of the enantiomer with the opposite configuration. (C) Additive favoring crystallization of the enantiomer with the same absolute configuration by forming an enantiospecific solid solution.

Chiral symmetry breaking is part and parcel of discussions of the origin of life.[1,2] In particular, complete symmetry breaking that led to homochirality in living organisms - exclusively L-amino acids and D-sugars - continues fascinating and puzzling scientists. However, despite tremendous efforts, the question "How this homochirality emerged?" remains open.

Enantiopure additives have been shown to direct the symmetry breaking in the Soai reaction to the same absolute configuration.[3],[4],[5] However, the mechanism of the Soai reaction is unique and its principles cannot be extended to prebiotic systems.

Symmetry breaking in solid phases has been studied in great detail for crystallization processes. Of particular interest is the case where nature has caused, for poorly understood reasons, crystallization of enantiomers as separate enantiomorphic phases (conglomerates) (Fig. 1A). Chiral additives have been shown to interact enantioselectively with racemic conglomerates in multiple ways, significantly influencing symmetry breaking processes. Additives can absorb stereospecifically on crystal surfaces and thereby inhibit the growth of the enantiomer of the same absolute configuration. Consequently, the solid phase becomes enriched in the enantiomer of the opposite absolute configuration to the additive (Fig. 1B). This well-known effect is the "rule of reversal" formulated by Lahav and Leiserowitz.[6,7]

Structurally and stereochemically similar molecules can also enantiospecifically incorporate into the bulk crystal lattice of enantiomorphs of the same absolute configuration to form a solid solution.[8–15] During crystallization, the enantiomorph does not distinguish between the enantiomer of the racemate and the corresponding additive. This phenomenon suggests that solid solution forming additives may be used to direct symmetry breaking in racemic solid phases of structurally related compounds towards the same, homochiral, absolute configuration. However, a powerful amplification mechanism is required to magnify the initially created imbalances.

We envisage that symmetry breaking induced by such enantiospecific solid solution formation followed by amplification favors propagation of the enantiomer of the same absolute configuration as the additive (Fig. 1C). This may serve as an experimental demonstration of how the absolute configuration of one compound can be transmitted to another one, thus offering a potential mechanism for propagation of homochirality.

We here demonstrate the validity of the above line of thought. As a first step, we identify suitable compounds that can form solid solutions and can undergo complete chiral symmetry breaking. Molecules that are similar by structure, size, and stereochemistry are known to crystallize as solid solutions.[12,13,16] Kitaigorodsky has introduced a coefficient of geometrical similarity $\varepsilon = 1 - V_{non\text{-}overlap}/V_{overlap}$, where $V_{non\text{-}overlap}$ and $V_{overlap}$ are non-overlapping and overlapping volumes of two superimposed molecules, respectively.[16] This geometrical coefficient can be used to quantify the degree of similarity of two molecules.[13,16–18] It has empirically been shown that the formation of a solid solution requires $0.8 < \varepsilon < 1$.[13,16,17] This suggests that molecules similar in size, decoration with substituents and absolute chirality, e.g.

10.1002/anie.202009719

family members, thus have a high probability to form homochiral solid solutions and thereby create enantioimbalances in both the liquid and solid phases.

To amplify these enantioimbalances we use Viedma ripening (i.e. attrition-induced deracemization) - a powerful method to amplify minute enantioimbalances to virtually absolute enantiomeric purity.[19–27] Viedma ripening requires racemizable conglomerates, *i.e* compounds that (a) crystallize as racemic conglomerates, and (b) racemize in the liquid phase, *i.e.* the enantiomers interconvert into one another.[28–31]

Based on the above analysis, we identified two families of compounds to test our hypothesis. Compounds **1a,b** and **2a,b** crystallize as conglomerates and undergo complete chiral symmetry breaking under Viedma ripening conditions.[32,33] Compounds **1b** and **2b** are family members of **1a** and **2a** respectively. Family members of the same absolute configuration (i.e. (*R*)-**1a,b**, (*S*)-**1a,b**, (*R*)-**2a,b** and (*S*)-**2a,b**) exhibit high geometrical similarities (for both pairs ((*S*)-**1a,b**) and ((*S*)-**2a,b**), $\varepsilon \approx 0.9$; SI),[13,16,17] suggesting a strong potential to form homochiral solid solutions.

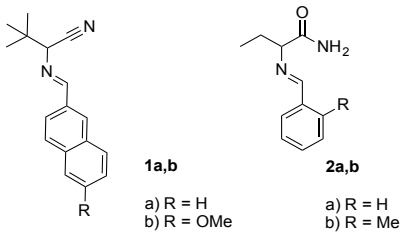

Scheme 1. Chemical structures of the two used families of compounds.

We investigated the enantiospecific solid solution formation with the family members **1a,b** and **2a,b.** Four mechanical mixtures of the additives and pure enantiomers of the racemates were prepared: (*S*)-**1a** + (*S*)-**1b**, (*R*)-**1a** + (*S*)-**1b**, (*S*)-**2a** + (*S*)-**2b** and (*R*)-**2a** + (*S*)-**2b** (SI). Solvents were added and the resulting slurries were sonicated in the presence of glass beads for 2 hours at 21 °C to enhance continuous growth/dissolution of crystals. Subsequently, the slurries were equilibrated for 16 hours at 21 °C. The liquid and solid phases were separated by filtration and the composition of both phases was analyzed by HPLC on a chiral column (Table 1, Table S1, SI). For both families of compounds, the enantiopure additive was incorporated into the solid phase of the same absolute configuration, (*S*)-**1b** + (*S*)-**1a**, and (*S*)-**2b** + (*S*)-**2a**), whereas no additive was incorporated into the solid phase of the opposite configuration. These observations indicate chiral discrimination *via* enantiospecific solid solution formation.

Structurally related molecules are also known to absorb on crystal surfaces.[7],[34],[35] Inspired by previous work of Lahav et al.,[36],[37] we performed a sequence of partial dissolution experiments to exclude that this absorption dominates in the observed enantioselective interactions (Table 1). We crystallized (*S*)-**1a** in the presence of approximately 10% (*S*)-**1b**. The resulting crystals were partly dissolved and the composition of the liquid phase was analyzed by HPLC. Partial dissolution experiments were repeated with the remaining solid phase until complete dissolution of the crystals (SI). The ratio of (*S*)-**1a** and (*S*)-**1b** in the collected liquid phases remained constant in all entries (Table S9, SI), suggesting that additive (*S*)-**1b** is homogeneously distributed through the crystals. The additive molecules are thus not only absorbed on crystal surfaces, but are rather homogeneously distributed in the bulk, consistent with solid solution formation.

Table 1. Enantiospecific interactions in families of conglomerates.

Starting mixture	Isolated solid
(*R*)-**1a** + (*S*)-**1b** (≈10 mol%)	(*R*)-**1a**
(*S*)-**1a** + (*S*)-**1b** (≈10 mol%)	(*S*)-**1a** + (*S*)-**1b** (3.1 mol%)
(*R*)-**2a** + (*S*)-**2b** (≈10 mol%)	(*R*)-**2a**
(*S*)-**2a** + (*S*)-**2b** (≈10 mol%)	(*S*)-**2a** + (*S*)-**2b** (1.5 mol%)

We also monitored the formation of solid solutions by X-ray powder diffraction analysis (XRPD). We prepared *homo*- ((*S*)-**a** with (*S*)-**b**) and *hetero*chiral ((*R*)-**a** with (*S*)-**b**) mixtures of family members containing approximately 10 mol% of the corresponding additive (SI). As expected, mixing crystals of family members without recrystallization, results in cumulative XRPD patterns of the pure compounds, regardless of their relative chiral configurations (Fig. S5 and Fig. S7, SI). However, XRPD patterns of the recrystallized mixtures clearly show difference between *homo*- and *hetero*chiral mixtures. After recrystallization of homochiral mixtures ((*S*)-**1a** with (*S*)-**1b**, and (*S*)-**2a** with (*S*)-**2b**), the characteristic diffraction peaks of the additive disappear, indicating incorporation of the additive into the crystal lattice of the homochiral family member to form a solid solution. Consequently, the lattice spacing of these crystals is slightly altered, which is consistent with the observed broadening and shifting of diffraction peaks (Fig. S6 and Fig. S8, SI). In contrast, recrystallization of *hetero*chiral mixtures ((*R*)-**1a** with (*S*)-**1b** and (*R*)-**2a** with (*S*)-**2b**) still yields XRPD patterns identical to their mechanical mixtures, thus indicating no incorporation of the additive into crystals of family members with the opposite absolute configuration.

Additionally, we performed an X-Ray diffraction analysis of a single crystal deposited from a MeOH solution of (*S*)-**1a** and (*S*)-**1b** in 10/1 weight ratio. The analysis revealed that the additive (*S*)-**1b** is indeed incorporated into the unit cell of (*S*)-**1a** (Fig. 2, SI). Upon incorporation, the hydrogen at the C9-atom is replaced by the OCH_3 -group (O91-C91). The refinement of the structure delivered a fixed occupation factor of 0.04 for the OCH_3 -group of the additive (*S*)-**1b**. Remarkably, the (*S*)-**1a** can be replaced by the additive (*S*)-**1b** without significant changes in the position of the molecule, and the unit cell volume only increases slightly from 1457.8 Å^3 ((*S*)-**1a**) to 1466.5 Å^3 ((*S*)-**1a**/(*S*)-**1b**). Collectively, these crystallographic studies confirm the enantiospecific formation of solid solutions of homochiral family members.

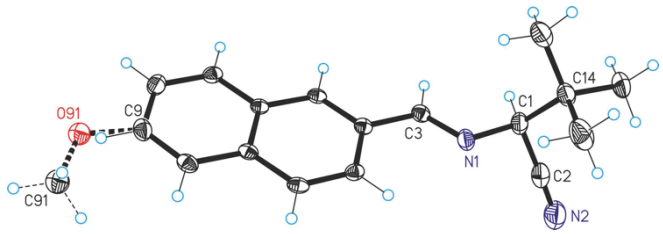

Figure 2. X-Ray diffraction analysis of a single crystal of the (*S*)-**1a**/(*S*)-**1b** solid solution deposited from MeOH. The methoxy group of incorporated (*S*)-**1b** is shown with dashed bonds.

We investigated if chiral discrimination via solid solution formation is sufficient to achieve symmetry breaking in racemic conglomerates. A slurry of the racemic conglomerate was sonicated for 2 hours at 21 °C in the presence of the enantiomerically pure additive. Subsequently, the slurry was equilibrated at 21 °C for 16 hours, the liquid and solid phases were

10.1002/anie.202009719

separated by filtration and analyzed by HPLC on a chiral column (Table S4, SI). To enable accurate determination of the absolute concentrations of each component in the liquid phase, stock solutions of internal standards were used in combination with calibration curves (Fig. 3, SI).

Analysis of the liquid phases showed that for the family members (*RS*)-**1a** and (*S*)-**1b**, the additive (*S*)-**1b** scarcely influences the solubility of (*R*)-**1a**. However, the concentration of (*S*)-**1a** decreases significantly (Fig. 3A). As a result, the solid phase enriches in (*S*)-**1a**. The presence of the enantiopure additive thus causes an enrichment of the solid phase in the same absolute configuration. A similar trend is observed for the family members of (*RS*)-**2a** and (*S*)-**2b**. Overall, solid phases enrich in the absolute configuration of the additive and liquid phases become enriched in the opposite configuration. Noteworthy, for **2a**, the absolute concentrations of both enantiomers **2a** as well as the absolute concentration of the additive (*S*)-**2b** increase, suggesting non-ideal solubility - the solubility of one component is influenced by the presence of another component (Fig. 3C). Consistently with these observations, addition of the corresponding racemic additive to (*RS*)-**1a** and (*RS*)-**2a** results in a decrease and increase of the liquid phase concentrations of both enantiomers, respectively (Fig. 3B, 3D). Enantiospecific interactions of additives with enantiomers of the same absolute configuration thus allow for manipulation of solid phase stabilities.

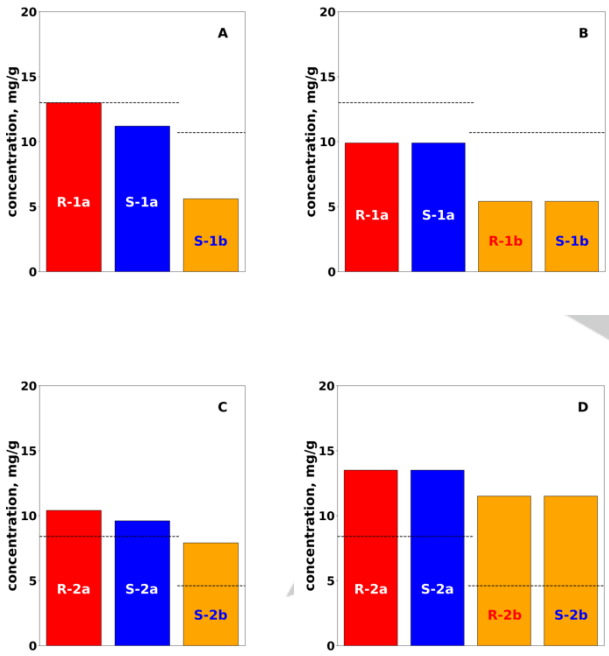

Figure 3. Absolute concentrations of the components in the liquid phase. (A) (*RS*)-**1a** and (*S*)-**1b**; (B) (*RS*)-**1a** and (*RS*)-**1b**; (C) (*RS*)-**2a** and (*S*)-**2b**; (D) (*RS*)-**1a** and (*RS*)-**2b**. Dashed lines are given for eye guidance and show separately measured solubilities of the corresponding components.

To amplify the initially created enantioimbalances, we used Viedma ripening. A slurry composed of a racemate and enantiomerically pure additive was sonicated in the presence of glass beads for 2 hours at 21 °C to ensure directed chiral symmetry breaking. Thereafter, 1,8-diazabicyclo[5.4.0]undec-7-ene (DBU) was added to initiate racemization in the liquid phase. The mixture was sonicated for 16 hours at 21 °C to achieve complete chiral symmetry breaking. HPLC analyses of the resulting solid phases showed that chiral symmetry breaking was directed towards the absolute configuration of the additive in all experiments (Table 2, Table S5, SI).

Table 2. Summary of the complete symmetry breaking experiments in the presence of a chiral additive.

Racemate	Additive	Outcome
(*RS*)-**1a**	(*R*)-**1b**	(*R*)-**1a**
(*RS*)-**1a**	(*S*)-**1b**	(*S*)-**1a**
(*RS*)-**1b**	(*R*)-**1a**	(*R*)-**1b**
(*RS*)-**1b**	(*S*)-**1a**	(*S*)-**1b**
(*RS*)-**2a**	(*R*)-**2b**	(*R*)-**2a**
(*RS*)-**2a**	(*S*)-**2b**	(*S*)-**2a**
(*RS*)-**2b**	(*R*)-**2a**	(*R*)-**2b**
(*RS*)-**2b**	(*S*)-**2a**	(*S*)-**2b**

These results demonstrate that the combination of enantiospecific solid solution formation and Viedma ripening provides complete chiral symmetry breaking towards the absolute configuration of the additive, thus offering a potential mechanism for the propagation of homochirality.

The present results are in contrast with the well-established “rule of reversal” in which symmetry breaking occurs towards the configuration that is opposite to the configuration of the additive. This phenomenon has been explained in terms of stereospecific absorption of the enantiomerically pure additive at the surface of the homochiral enantiomorph. Consequently, the growth of this enantiomorph is inhibited, with the result that the opposite enantiomer crystallizes preferentially.

Stereospecific growth inhibition is kinetically driven,[7] whereas solid solutions formation is thermodynamically controlled. Even though we observe solid solution behavior for both families of compounds, there may still be a time-dependent signature of enantiospecific growth inhibition. To understand if enantiospecific growth inhibition occurs with solid solution forming systems, we investigated the initial symmetry breaking process in time. To this aim, we ground slurries of the racemic conglomerates and corresponding additives ((*RS*)-**1a** + (*S*)-**1b** and (*RS*)-**1a** + (*S*)-**1b**) and monitored the compositions of the liquid and solid phases over time (Fig. 4, Fig. S10, SI). In both families, chiral symmetry breaking occurs as soon as we initiate grinding in the presence of the corresponding additive. Remarkably, with (*RS*)-**1a**, the solid phase first enriches in the chiral configuration (*R*)-**1a** that is opposite to the configuration of the additive (*S*)-**1b** (Fig. 4A). This initial symmetry breaking is thus consistent with the “rule-of-reversal”: the additive inhibits growth of the homochiral enantiomorph. However, after ca. 120 minutes, a sudden drop in the absolute concentration of the additive (*S*)-**1b** is observed, suggesting the formation of the solid solution (Fig. 4B). Simultaneously, the liquid and solid phases of the slurry switch their “signs” of chirality: the solid phase becomes enriched in the configuration (*S*)-**1a**, identical to the additive (*S*)-**1b**, while the liquid phase becomes enriched in opposite enantiomer (*R*)-**1a** (Fig. 4A). These abrupt changes directly visualize the transition between the two symmetry breaking processes: initially kinetic growth inhibition dominates, but in the end, thermodynamically controlled solid solution formation overrules. This enantioimbalance remains preserved once grinding is stopped, even after 3 months, thus confirming the thermodynamic nature of this stage of symmetry breaking.

10.1002/anie.202009719

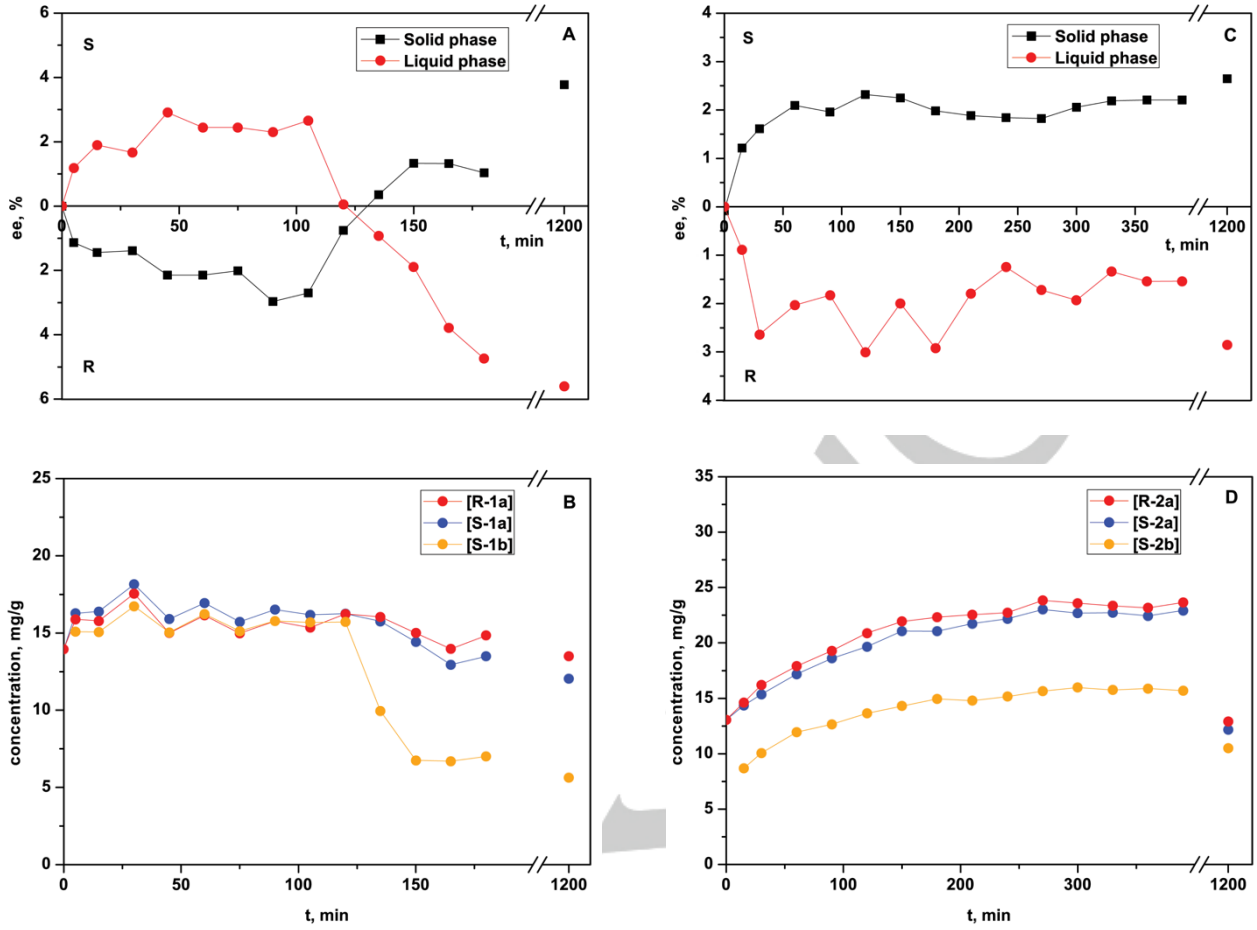

Figure 4. Time-resolved symmetry breaking in the presence of an enantiopure additive. (A) Enantiomeric excess evolution in (*RS*)-**1a** liquid (blue) and solid (red) phases in the presence of (*S*)-**1b**, and (B) absolute concentration of the liquid phase components during the symmetry breaking of (*RS*)-**1a**. (C) Enantiomeric excess evolution in (*RS*)-**2a** liquid (blue) and solid (red) phases in the presence of (*S*)-**2b**, and (D) absolute concentration of the liquid phase components during the symmetry breaking of (*RS*)-**2a**. Note: the data points at 1200 min correspond to the analyses of the equilibrated mixtures.

On the other hand, for (*RS*)-**2a** with (*S*)-**2b** as additive, chiral symmetry breaking evolves directly towards the absolute configuration of the additive, and no switch in the sign of chirality is observed (Fig. 4C). The absence of this switch may be explained in terms of the increased solubility of (*RS*)-**2a** in the presence of (*S*)-**2b** (Fig. 2C, 2D). Indeed, the solution concentration increases in time due to dissolution (Fig. 4D). Enantiospecific dissolution inhibition causes solid phase enantioenrichment in the absolute configuration of the additive,[7,38] and might initially be the dominant process during symmetry breaking. However, in this case, both phenomena—e nantiospecific solid solution formation and enantiospecific dissolution inhibition—favor the same outcome of the symmetry breaking, and we are therefore unable to distinguish between dominant contributions of the kinetic and thermodynamic processes for (*RS*)-**2a**.

Our observations help to understand the causes of some discrepancies observed during studies of symmetry breaking processes. In particular, the fact that deracemization of racemic 1,1'-binaphthyl in the presence enantiomerically pure 1,1'-bi-2-naphthol does not follow the rule of reversal,[39] can be explained in terms of a homochiral solid solution between 1,1'-binaphthyl and 1,1'-bi-2-naphthol.

In summary, our findings offer a potential mechanism of the propagation of homochirality using compounds derived from the pre-biologically relevant Strecker syntheses. We demonstrate that a single chiral additive can direct initial chiral symmetry breaking to opposite outcomes. We identify two processes: kinetically driven growth inhibition directs symmetry breaking towards the opposite enantiomer, whereas thermodynamically controlled solid solution formation favors the homochiral outcome. The relative contributions of these antagonistic processes may be rationally balanced by the crystallization conditions. These insights thus offer a new playground for controlling symmetry breaking processes that are of fundamental and practical importance.

Acknowledgements

The authors are grateful for inspiring and fruitful discussions with Dr. Bernard Kaptein. This work was supported by AMOLF funds for Topsector-related research and IXAnext Physics2Market grant.

Keywords: chiral symmetry breaking • homochirality • solid solution • deracemization • crystallization

[1] J. L. Bada, *Nature* **1995**, *374*, 594–595.
[2] J. L. Bada, *Chem. Soc. Rev.* **2013**, *42*, 2186–2196.
[3] F. C. Frank, *Biochim. Biyphysica Acta* **1953**, *11*, 459–463.
[4] K. Soai, T. Shibata, H. Morloka, K. Choji, *Nature* **1995**, *378*, 767–768.
[5] N. A. Hawbaker, D. G. Blackmond, *Nat. Chem.* **2019**, *11*, 957–962.
[6] L. Addadi, Z. Berkovitch Yellin, N. Domb, E. Gati, M. Lahav, L. Leiserowitz, *Nature* **1982**, *296*, 21–26.
[7] L. Addadi, S. Weinstein, E. Gati, I. Weissbuch, M. Lahav, *J. Am. Chem. Soc.* **1982**, *104*, 4610–4617.
[8] S. Kojo, K. Tanaka, *Chem. Commun.* **2001**, *1*, 1980–1981.
[9] S. Kojo, H. Uchino, M. Yoshimura, K. Tanaka, *Chem. Commun.* **2004**, *10*, 2146–2147.
[10] N. Liu, S. Haq, G. R. Darling, R. Raval, *Angew. Chemie - Int. Ed.* **2007**, *46*, 7613–7616.
[11] M. Leeman, J. M. De Gooier, K. Boer, K. Zwaagstra, B. Kaptein, R. M. Kellogg, *Tetrahedron Asymmetry* **2010**, *21*, 1191–1193.
[12] C. Garcia, A. Collet, *Tetrahedron: Asymmetry* **1992**, *3*, 361–364.
[13] A. Collet, L. Ziminski, C. Garcia, F. Vigné-Maeder, in *Supramol. Stereochem.*, Springer Netherlands, Dordrecht, **1995**, pp. 91–110.
[14] M. Vaida, L. J. W. Shimon, Y. Weisinger-Lewin, F. Frolow, M. Lahav, L. Leiserowitz, R. K. McMullan, *Science.* **1988**, *241*, 1475–1479.
[15] J. M. McBride, *Angew. Chemie Int. Ed.* **1989**, *28*, 377–379.
[16] A. I. Kitaigorodsky, *Organic Chemical Crystallography*, Consultants Bureau, New York, USA, **1961**.
[17] A. I. Kitaigorodsky, *Mixed Crystals*, Springer-Verlag, Berlin Heidelberg, **1984**.
[18] *Kitaigorodskiy's Similarity Coefficient Is Essentially Geometrical and Does Not Take into Account the Nature of Chemical Interactions in the Crystal.*, **n.d.**
[19] C. Viedma, *Phys. Rev. Lett.* **2005**, *94*, 065504.
[20] W. L. Noorduin, T. Izumi, A. Millemaggi, M. Leeman, H. Meekes, W. J. P. Van Enckevort, R. M. Kellogg, B. Kaptein, E. Vlieg, D. G. Blackmond, *J. Am. Chem. Soc.* **2008**, *130*, 1158–1159.
[21] W. L. Noorduin, W. J. P. van Enckevort, H. Meekes, B. Kaptein, R. M. Kellogg, J. C. Tully, J. M. McBride, E. Vlieg, *Angew. Chem. Int. Ed.* **2010**, *49*, 8435–8438.
[22] C. Viedma, J. E. Ortiz, T. De Torres, T. Izumi, D. G. Blackmond, *J. Am. Chem. Soc.* **2008**, *130*, 15274–15275.
[23] L.-C. Sögütoglu, R. E. Steendam, H. Meekes, E. Vlieg, F. P. J. T. Rutjes, *Chem. Soc. Rev.* **2015**, *44*, 6723–6732.
[24] W. L. Noorduin, H. Meekes, A. A. C. Bode, W. J. P. Van Enckevort, B. Kaptein, R. M. Kellogg, E. Vlieg, *Cryst. Growth Des.* **2008**, *8*, 1675–1681.
[25] A. Matsumoto, Y. Kaimori, M. Uchida, H. Omori, T. Kawasaki, K. Soai, *Angew. Chemie - Int. Ed.* **2017**, *56*, 545–548.
[26] T. P. T. Nguyen, P. S. M. Cheung, L. Werber, J. Gagnon, R. Sivakumar, C. Lennox, A. Sossin, Y. Mastai, L. A. Cuccia, *Chem. Commun.* **2016**, *52*, 12626–12629.
[27] G. Belletti, C. Tortora, I. D. Mellema, P. Tinnemans, H. Meekes, F. P. J. T. Rutjes, S. B. Tsogoeva, E. Vlieg, *Chem. - A Eur. J.* **2020**, *26*, 839–844.
[28] C. Rougeot, F. Guillen, J.-C. Plaquevent, G. Coquerel, *Cryst. Growth Des.* **2015**, *15*, 2151–2155.
[29] P. Wilmink, C. Rougeot, K. Wurst, M. Sanselme, M. Van Der Meijden, W. Saletra, G. Coquerel, R. M. Kellogg, *Org. Process Res. Dev.* **2015**, *19*, 302–308.
[30] N. Uemura, S. Toyoda, H. Ishikawa, Y. Yoshida, T. Mino, Y. Kasashima, M. Sakamoto, *J. Org. Chem.* **2018**, *83*, 9300–9304.
[31] I. Baglai, M. Leeman, B. Kaptein, R. M. Kellogg, W. L. Noorduin, *Chem. Commun.* **2019**, *55*, 6910–6913.
[32] I. Baglai, M. Leeman, R. M. Kellogg, W. L. Noorduin, *Org. Biomol. Chem.* **2019**, *17*, 35–38.
[33] I. Baglai, M. Leeman, K. Wurst, B. Kaptein, R. M. Kellogg, W. L. Noorduin, *Chem. Commun.* **2018**, *54*, 10832–10834.
[34] I. Weissbuch, L. Addadi, Z. B. Yellin, E. Gati, S. Weinstein, M. Lahav, L. Leiserowitz, *J. Am. Chem. Soc.* **1983**, *105*, 6615–6621.
[35] E. Meirzadeh, I. Azuri, Y. Qi, D. Ehre, A. M. Rappe, M. Lahav, L. Kronik, I. Lubomirsky, *Nat. Commun.* **2016**, *7*, 13351.
[36] L. J. W. Shimon, D. Zbaida, L. Addadi, L. Leiserowitz, M. Lahav, *Mol. Cryst. Liq. Cryst. Inc. Nonlinear Opt.* **1988**, *161*, 199–221.
[37] L. J. W. Shimon, M. Lahav, L. Leiserowitz, *J. Am. Chem. Soc.* **1985**, *107*, 3375–3377.
[38] W. L. Noorduin, H. Meekes, W. J. P. Van Enckevort, B. Kaptein, R. M. Kellogg, E. Vlieg, *Angew. Chem. Int. Ed.* **2010**, *49*, 2539–2541.
[39] A. H. J. Engwerda, P. Van Schayik, H. Jagtenberg, H. Meekes, F. P. J. T. Rutjes, E. Vlieg, *Chem. Eur. J.* **2018**, *24*, 2863–2867.

10.1002/anie.202009719

WILEY-VCH

COMMUNICATION

Entry for the Table of Contents

Insert graphic for Table of Contents here.

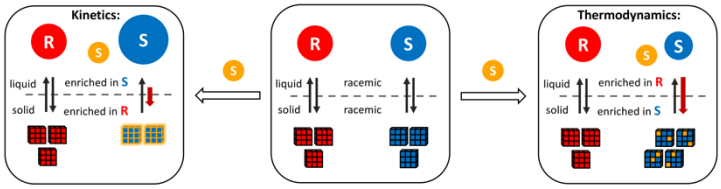

A single enantiomerically pure additive can direct chiral symmetry breaking process towards opposite outcomes, depending on relative contributions of *kinetic* and *thermodynamic* processes. Kinetic growth inhibition directs symmetry breaking in the solid phase towards the enantiomer of the opposite configuration to the additive, whereas thermodynamic solid solution formation favors the same absolute configuration, thus offering a potential mechanism for propagation of homochirality.

Institute and/or researcher Twitter usernames: ((optional))